

## PROBING NEW PHYSICS IN B PENGUINS \* †

J.L. HEWETT

*Stanford Linear Accelerator Center  
Stanford University, Stanford, CA 94309*

### ABSTRACT

Constraints placed on physics beyond the Standard Model from the recent CLEO observation of the inclusive decay  $B \rightarrow X_s \gamma$  are summarized. Further searches for new physics using the process  $B \rightarrow X_s \ell^+ \ell^-$  are discussed.

The study of virtual effects can open an important window on electroweak symmetry breaking and physics beyond the Standard Model (SM). The examination of indirect effects of new physics in higher order processes offers a complementary approach to the search for direct production of new particles at high energy colliders. In fact, tests of loop induced couplings can provide a means of probing the detailed structure of the SM at the level of radiative corrections where Glashow-Iliopoulos-Maiani (GIM) cancellations are important. In some cases the constraints on new degrees of freedom via indirect effects surpass those obtainable from collider searches. In other cases, entire classes of models are found to be incompatible. Given the amount of high luminosity data on the  $B$  system which will become available during the next decade, this approach to searching for physics beyond the SM will become an increasingly valuable tool.

Radiative  $B$  decays have become one of the best testing grounds of the SM due to recent progress on both the experimental and theoretical fronts. The CLEO Collaboration has recently reported[1] the observation of the inclusive decay  $B \rightarrow X_s \gamma$  with a branching fraction of  $(2.32 \pm 0.57 \pm 0.35) \times 10^{-4}$ . Observation of this process at the inclusive level removes the uncertainties associated with folding in the imprecisely predicted[2] ratio of exclusive to inclusive rates when comparing theoretical results with exclusive data. On the theoretical side, the reliability of the calculation of the quark-level process  $b \rightarrow s \gamma$  is improving[3] as agreement on the leading-logarithmic QCD corrections has been reached and partial calculations at the next-to-leading logarithmic order are underway. These new results have inspired a large number of investigations of this decay in various classes of models, which can be summarized by the following list:

---

\*Work Supported by the Department of Energy, Contract DE-AC03-76SF00515

†Presented at the *International Workshop on B Physics: Physics Beyond the Standard Model at the B Factory*, Nagoya, Japan, October 26-28, 1994

- “Top Ten” Models Probed by  $b \rightarrow s\gamma$

- |  |                                 |
|--|---------------------------------|
| 1. Standard Model                      | 6. Supersymmetry                |
| 2. Anomalous Top-Quark Couplings       | 7. Three-Higgs-Doublet Model    |
| 3. Anomalous Trilinear Gauge Couplings | 8. Extended Technicolor         |
| 4. Fourth Generation                   | 9. Leptoquarks                  |
| 5. Two-Higgs-Doublet Models            | 10. Left-Right Symmetric Models |

Clearly, I only have time to discuss a couple of these models here, a more complete review can be found in Ref. [4].

In the SM, the quark-level transition  $b \rightarrow s\gamma$  is mediated by  $W$ -boson and  $t$ -quark exchange in an electromagnetic penguin diagram. To obtain the branching fraction, the inclusive rate is scaled to that of the semi-leptonic decay  $b \rightarrow X\ell\nu$ . This procedure removes uncertainties in the calculation due to an overall factor of  $m_b^5$  which appears in both expressions, and reduces the ambiguities involved with the imprecisely determined Cabibbo-Kobayashi-Maskawa (CKM) factors. The result is then rescaled by the experimental value[5] of  $B(b \rightarrow X\ell\nu)$ . The semi-leptonic rate is calculated incorporating both charm and non-charm modes, and includes both phase space and QCD corrections[6]. The calculation of  $\Gamma(b \rightarrow s\gamma)$  employs the renormalization group evolution[3] for the coefficients of the  $b \rightarrow s$  transition operators in the effective Hamiltonian at the leading logarithmic level. The participating operators consist of the current-current operators  $O_{1,2}$ , the QCD penguin operators  $O_{3-6}$ , and the electro- and chromo-magnetic operators  $O_{7,8}$ . The Wilson coefficients of the  $b \rightarrow s$  operators are evaluated perturbatively at the  $W$  scale, where the matching conditions are imposed, and evolved down to the renormalization scale  $\mu$ , usually taken to be  $\sim m_b$ . This procedure yields the branching fraction  $B(b \rightarrow s\gamma) = 2.92_{-0.59}^{+0.77} \times 10^{-4}$  for a top-quark mass of 175 GeV. The central value corresponds to  $\mu = m_b$ , while the upper and lower errors represent the deviation due to assuming  $\mu = m_b/2$  and  $\mu = 2m_b$ , respectively. We see that (i) this value compares favorably to the recent CLEO measurement and (ii) the freedom of choice in the value of the renormalization scale introduces an uncertainty of order 25 – 30%. Clearly, when determining constraints on new physics from this process, one must choose values for the parameters which yield the most conservative limits.

Before discussing explicit models of new physics, we first investigate the constraints placed directly on the Wilson coefficients of the magnetic moment operators. Writing the coefficients at the matching scale in the form  $c_i(M_W) = c_i(M_W)_{SM} + c_i(M_W)_{new}$ , where  $c_i(M_W)_{new}$  represents the contributions from new interactions, we see that the CLEO measurement limits the possible values of  $c_i(M_W)_{new}$  for  $i = 7, 8$ . These bounds are presented in Fig. 1(a), for  $m_t = 175$  GeV, where the allowed regions lie inside the diagonal bands. We note that the two bands occur due to the overall sign ambiguity in the determination of the coefficients (recall that  $B(b \rightarrow s\gamma) \propto |c_7^{eff}(\mu)|^2$ ), and by including the upper and lower CLEO bounds. The horizontal lines correspond

to potential limits  $B(b \rightarrow sg) < (3-30) \times B(b \rightarrow sg)_{SM}$ . We see that such a constraint on  $b \rightarrow sg$  is needed to further restrict the values of the Wilson coefficients.

The trilinear gauge coupling of the photon to  $W^+W^-$  can be tested in  $b \rightarrow s\gamma$  decay. Anomalous  $\gamma WW$  vertices can be probed by looking for deviations from the SM in tree-level processes such as  $e^+e^- \rightarrow W^+W^-$  and  $p\bar{p} \rightarrow W\gamma$ , or by their influence on loop order processes, for example the  $g-2$  of the muon. In the latter case, cutoffs must be used in order to regulate the divergent loop integrals and can introduce errors by attributing a physical significance to the cutoff[7]. However, some loop processes, such as  $b \rightarrow s\gamma$ , avoid this problem due to cancellations provided by the GIM mechanism, and hence yield cutoff independent bounds on anomalous couplings. The CP-conserving interaction Lagrangian for  $WW\gamma$  interactions is

$$\mathcal{L}_{WW\gamma} = i \left( W_{\mu\nu}^\dagger W^\mu A^\nu - W_\mu^\dagger A_\nu W^{\mu\nu} \right) + i\kappa_\gamma W_\mu^\dagger W_\nu A^{\mu\nu} + i\frac{\lambda_\gamma}{M_W^2} W_{\lambda\mu}^\dagger W_\nu^\mu A^{\nu\lambda}, \quad (1)$$

where  $V_{\mu\nu} = \partial_\mu V_\nu - \partial_\nu V_\mu$ , and the two parameters  $\kappa_\gamma = 1 + \Delta\kappa_\gamma$  and  $\lambda_\gamma$  take on the values  $\Delta\kappa_\gamma, \lambda_\gamma = 0$  in the SM. In this case, only the coefficient of the magnetic dipole operator,  $O_7$ , is modified by the presence of these additional terms and can be written as

$$c_7(M_W) = G_7^{SM}(m_t^2/M_W^2) + \Delta\kappa_\gamma A_1(m_t^2/M_W^2) + \lambda_\gamma A_2(m_t^2/M_W^2). \quad (2)$$

The explicit form of the functions  $A_{1,2}$  can be found in Ref. [8]. As both of these parameters are varied, either large enhancements or suppressions over the SM prediction for the  $b \rightarrow s\gamma$  branching fraction can be obtained. When one demands consistency with both the upper and lower CLEO bounds, a large region of the  $\Delta\kappa_\gamma - \lambda_\gamma$  parameter plane is excluded; this is displayed in Fig. 1(b) from Ref. [1] for  $m_t = 174$  GeV. Here, the allowed region is given by the cross-hatched area, where the white strip down the middle is excluded by the lower bound and the outer white areas are ruled out by the upper limit on  $B(b \rightarrow s\gamma)$ . The ellipse represents the region allowed by D0[9]. Note that the SM point in the  $\Delta\kappa_\gamma - \lambda_\gamma$  plane (labeled by the dot) lies in the center of one of the allowed regions. We see that the collider constraints are complementary to those from  $b \rightarrow s\gamma$ .

Next we turn to two-Higgs-doublet models (2HDM), where we examine the case (denoted as Model II) where the second doublet,  $\phi_2$ , gives mass to the up-type quarks, while the down-type quarks and charged leptons receive their mass from  $\phi_1$ . Each doublet obtains a vacuum expectation value (vev)  $v_i$ , subject to the constraint that  $v_1^2 + v_2^2 = v^2$ , where  $v$  is the usual vev present in the SM. The charged Higgs boson interactions with the quark sector are governed by the Lagrangian

$$\mathcal{L} = \frac{g}{2\sqrt{2}M_W} H^\pm \left[ V_{ij} m_{u_i} A_u \bar{u}_i (1 - \gamma_5) d_j + V_{ij} m_{d_j} A_d \bar{u}_i (1 + \gamma_5) d_j \right] + H.c., \quad (3)$$

where  $g$  is the usual SU(2) coupling constant and  $V_{ij}$  represents the appropriate CKM element. In Model II,  $A_u = \cot \beta$  and  $A_d = \tan \beta$ , where  $\tan \beta \equiv v_2/v_1$  is the ratio of

vevs. The  $H^\pm$  contributes to  $b \rightarrow s\gamma$  via virtual exchange together with the top-quark and the dipole  $b \rightarrow s$  operators ( $O_{7,8}$ ) receive contributions from this exchange. At the  $W$  scale the coefficients of these operators take the form

$$c_i(M_W) = G_i^{SM}(m_t^2/M_W^2) + A_{1_i}^{H^\pm}(m_t^2/m_{H^\pm}^2) + \frac{1}{\tan^2\beta}A_{2_i}^{H^\pm}(m_t^2/m_{H^\pm}^2), \quad (4)$$

where  $i = 7, 8$ . The analytic form of the functions  $A_{1_i}, A_{2_i}$  can be found in [10]. In Model II, large enhancements appear for small values of  $\tan\beta$ , but more importantly, we see that  $B(b \rightarrow s\gamma)$  is always larger than that of the SM, independent of the value of  $\tan\beta$  due to the presence of the  $A_{1_i}^{H^\pm}$  term. In this case, the CLEO upper bound excludes[1, 11] the region to the left and beneath the curves shown in Fig. 1(c) for  $m_t = 174 \pm 16$  GeV and  $\mu = 2m_b$ . We note that the  $H^\pm$  couplings present in Model II are of the type present in Supersymmetry. However, the limits obtained in supersymmetric theories also depend on the size of the other super-particle contributions to  $b \rightarrow s\gamma$ , and are generally much more complex[12, 13].

The inclusive process  $b \rightarrow s\ell^+\ell^-$  also offers an excellent opportunity to search for new physics. The decay proceeds via electromagnetic and  $Z$  penguin as well as by  $W$  box diagrams, and hence can probe different coupling structures than the pure electromagnetic process  $b \rightarrow s\gamma$ . This reaction also receives long distance contributions from the processes  $B \rightarrow K^{(*)}\psi^{(\prime)}$  followed by  $\psi^{(\prime)} \rightarrow \ell^+\ell^-$  and from  $c\bar{c}$  continuum intermediate states. The short distance contributions lead to the inclusive branching fractions[14] (including the leading logarithmic QCD corrections)  $B(B \rightarrow X_s\ell^+\ell^-) \sim (15, 7, 2) \times 10^{-6}$  for  $\ell = (e, \mu, \tau)$ , respectively, and hence these modes will likely be observed during the next few years. The best method of separating the long and short distance contributions, as well as observing any deviations from the SM, is to measure the various kinematic distributions associated with the final state lepton pair, such as the lepton pair invariant mass distribution[14], the lepton pair forward-backward asymmetry[15], and the tau polarization asymmetry[16] in the case  $\ell = \tau$ . Measurement of all these quantities would allow for the determination of the sign and magnitude of the Wilson coefficients for the electroweak loop operators and thus provide a completely model independent analysis. We note that measurement of these distributions requires the high statistics samples which will be available at future B-factories. The lepton pair invariant mass distribution for  $b \rightarrow se^+e^-$  is displayed in Fig. 3(a) (taking  $m_t = 175$  GeV), where the solid curve includes the contributions from the short and long range effects and the dashed curve represents the short distance alone. We see that the long distance contributions dominate only in the  $M_{e^+e^-}$  regions near the  $\psi$  and  $\psi'$  resonances, and observations away from these peaks would cleanly separate the short distance physics. The tau polarization asymmetry is presented in Fig. 3(b); we see that it is large and negative for this value of  $m_t$ . As an example of how new physics can affect this process, we examine  $b \rightarrow s\ell^+\ell^-$  in the case of an anomalous  $WW\gamma$  vertex. The resulting invariant mass spectrum is shown in Fig. 3(c) for several values of  $\Delta\kappa_\gamma$  (taking  $\lambda_\gamma = 0$ ), and the variation of the

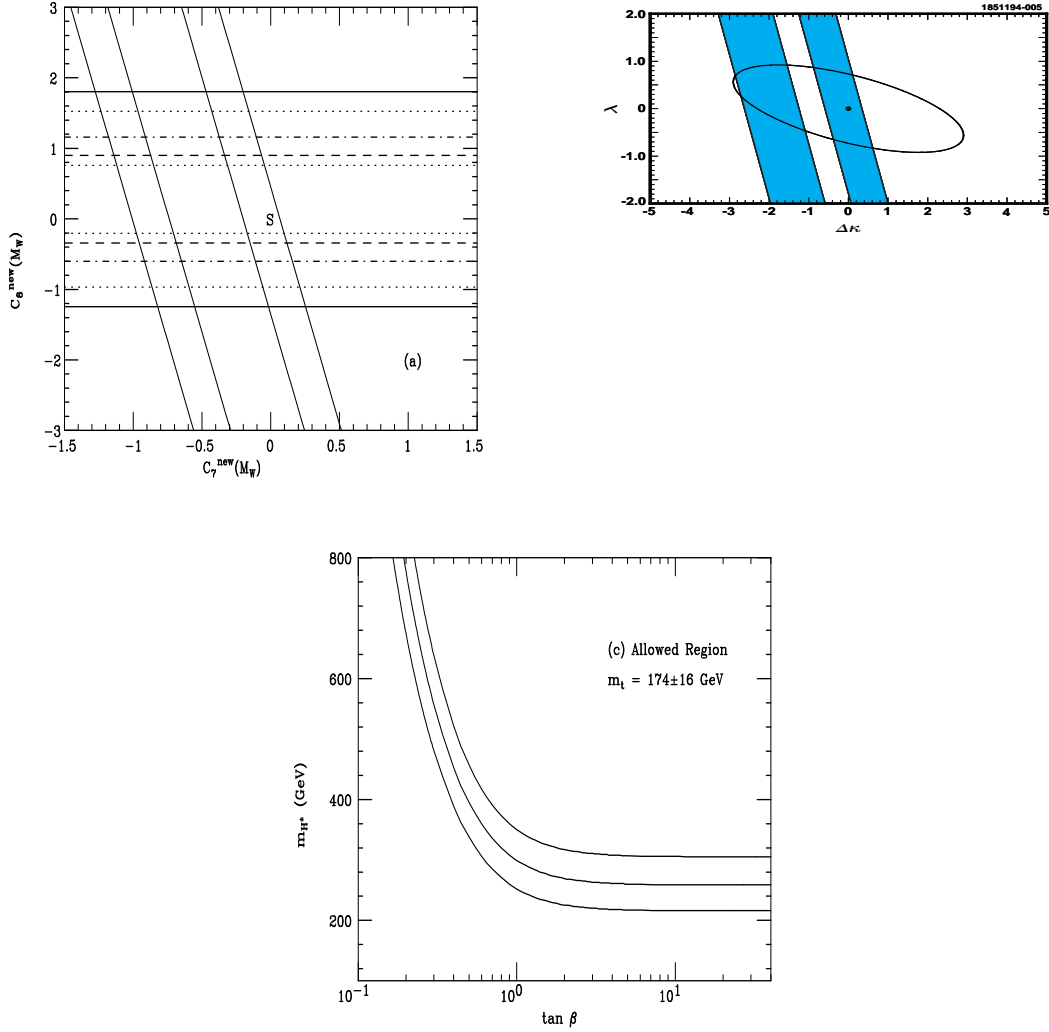


Figure 1: (a) Bounds on the contributions from new physics to  $c_{7,8}$ . The region allowed by CLEO corresponds to the area inside the diagonal bands. The horizontal lines represent potential measurements of  $R \equiv B(b \rightarrow sg)/B(b \rightarrow sg)_{SM} < 30, 20, 10, 5, 3$  corresponding to the set of solid, dotted, dash-dotted, dashed, and dotted lines, respectively. The point ‘S’ represents the SM. (b) Constraints on anomalous  $WW\gamma$  couplings. The shaded area is that allowed by CLEO and the interior of the ellipse is the region allowed by D0. The dot represent the SM values. (c) Limits from  $b \rightarrow s\gamma$  in the charged Higgs mass -  $\tan \beta$  plane. The excluded region is that to the left and below the curves. The three curves correspond to the values  $m_t = 190, 174, 158$  GeV from top to bottom.

tau polarization asymmetry with non-zero values of  $\Delta\kappa_\gamma$  and  $\lambda_\gamma$  is displayed in Fig. 3(d) for  $\hat{s} \equiv q^2/m_b^2 = 0.7$ .

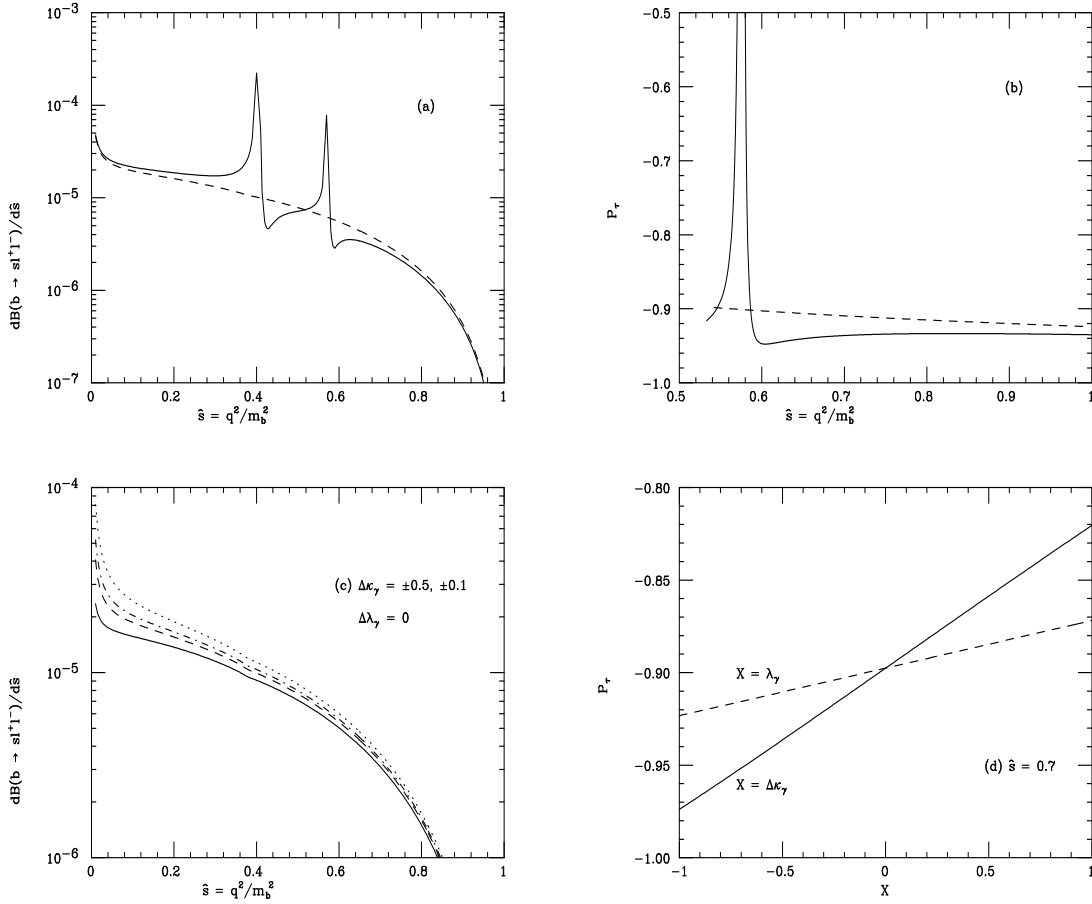


Figure 2: The (a) lepton pair mass distribution (with  $\ell = e$ ) and (b) tau polarization asymmetry (with  $\ell = \tau$ ) in the SM, and the (c) lepton pair mass distribution and (d) tau polarization asymmetry with anomalous  $WW\gamma$  couplings as labeled, for the process  $b \rightarrow sl^+\ell^-$  with  $m_t = 175$  GeV.

In summary, we have seen that the process  $b \rightarrow s\gamma$  provides powerful constraints for a variety of models containing physics beyond the SM. In most cases, these constraints either complement or are stronger than those from other low-energy processes and from direct collider searches. The decay  $b \rightarrow sl^+\ell^-$  is also an excellent probe of new physics. It is sensitive to possible new interactions since it allows the investigation of various kinematic distributions. Measurement of these quantities would allow for the determination of the sign and magnitude of all the contributing Wilson coefficients. We see that rare  $B$  decays add powerful insight to the quest for physics beyond the SM.

## References

1. M.S. Alam *et al.*, (CLEO Collaboration), Phys. Rev. Lett. **74**, 2885 (1995).
2. C. Bernard, P. Hsieh, and A. Soni, Phys. Rev. Lett. **72**, 1402 (1994).
3. A.J. Buras *et al.*, Nucl. Phys. **B424**, 374 (1994), and references therein.
4. J.L. Hewett, talk presented at the *XXI SLAC Summer Institute*, July 26 - August 6, 1993, Stanford, CA, SLAC-PUB-6521.
5. Particle Data Group, L. Montanet *et al.*, Phys. Rev. **D50**, 1173 (1994).
6. N. Cabibbo and L. Maiani, Phys. Lett. **B79**, 109 (1978).
7. C.P. Burgess and D. London, Phys. Rev. Lett. **69**, 3428 (1992); Phys. Rev. **D48**, 4337 (1993).
8. T.G. Rizzo, Phys. Lett. **B315**, 471 (1993); S.-P. Chia, Phys. Lett. **B240**, 465 (1990); K.A. Peterson, Phys. Lett. **B282**, 207 (1992).
9. J. Ellison (D0 Collaboration), Proceeding of *1994 Meeting of the Division of Particles and Fields*, Albuquerque, NM (1994). For comparable bounds from CDF and UA2, see F. Abe *et al.*, (CDF Collaboration) Phys. Rev. Lett. **74**, 1936 (1995); J. Alitti *et al.*, UA2 Collaboration, Phys. Lett. **B277**, 194 (1992).
10. T.G. Rizzo, Phys. Rev. **D38**, 820 (1988); W.-S. Hou and R.S. Willey, Phys. Lett. **B202**, 591 (1988); C.Q. Geng and J.N. Ng, Phys. Rev. **D38**, 2858 (1988); B. Grinstein, R. Springer, and M. Wise, Nucl. Phys. **B339**, 269 (1990); V. Barger, J.L. Hewett, and R.J.N. Phillips, Phys. Rev. **D41**, 3421 (1990).
11. J.L. Hewett, Phys. Rev. Lett. **70**, 1045 (1993); V. Barger, M. Berger, and R.J.N. Phillips, Phys. Rev. Lett. **70**, 1368 (1993).
12. S. Bertolini, *et al.*, Nucl. Phys. **B294**, 321 (1987), and Nucl. Phys. **B353**, 591 (1991).
13. Y. Okada, these proceedings.
14. N.G. Deshpande and J. Trampetic, Phys. Rev. Lett. **60**, 2583 (1988); C.S. Lim, T. Morozumi, and A.I. Sanda, Phys. Lett. **B218**, 343 (1989); N.G. Deshpande, J. Trampetic, and K. Panrose, Phys. Rev. **D39**, 1461 (1989); B. Grinstein, M.J. Savage, and M.B. Wise, Nucl. Phys. **B319**, 271 (1989).
15. A. Ali, these proceedings; A. Ali, G.F. Guidice, and T. Mannel CERN Report CERN-TH.7346/94; A. Ali, T. Mannel, and T. Morozumi, Phys. Lett. **B273**, 505 (1991).
16. J.L. Hewett, SLAC Report, SLAC-PUB-95-6820.